CHAPTER 2

THEORETICAL REVIEW

To facilitate the understanding of structure of elementary constituents of matter, various quark models have been developed. The Standard Model has been used successfully to describe the existing leptons and quarks within hadrons. In probing the interactions within hadrons, several theories such as the Quark Parton Model (QPM), the Quantum Chromodynamics (QCD), Lund String Fragmentation and Boson Gluon Fusion (BGF) have been used together with the kinematics variables of electron-proton collision to explain the existence of strong and weak interaction within the matter. In this chapter, the various theories involved in kinematics of the long-lived neutral hadrons in the calorimeter of the ZEUS detector were reviewed

2.1 The Standard Model

In high energy physics, research on the structure of elementary constituents of matter and the interaction of radiation with matter is carried out to understand the mechanism of hadrons being

bound within the nucleus. The standard model classifies elementary constituents of matter into six leptons and six quarks. The six leptons are electrons (e), muon (μ), tau (τ), electron neutrino (ν_e), muon neutrino (ν_μ) and tau neutrino (ν_τ), while the six quarks, also known as flavors, are up quark (u), down quark (d), charm quark (c), strange quark (s), top quark (t) and bottom quark (b).

As fermions, leptons are free particles that can be detected, but quarks on the other hand exist in bound states as hadrons and can only be inferred from experimental measurements of the properties of particle interactions and hadron productions [21].

The exchanges of field quanta between these fundamental constituents are governed by three forces –weak, electromagnetic and strong. These forces are mediated by carriers of forces called bosons that comprise of three vector boson mediating weak interactions ($W^{\pm}, Z^0$), the photon γ mediating electromagnetic and eight gluons mediating the strong interactions. Due to this gluon-gluon force, the quarks are confined within composite particles call hadrons that limit strong interaction to 10^{-15} meters.

As most of the elementary particle do not exist stably outside the confinement of hadrons, but created and detected during energetic collision with other particles, accelerator such as HERA was used as experimental tool to extract information on the kinematic variables of the elementary particles during their creation process.

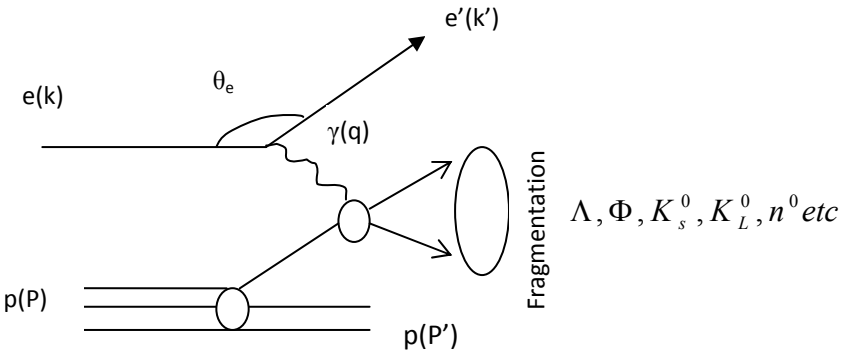

Figure 2.1 Kinematic variables in the electron-proton collision, with P, k , q as the momentum of proton, electron, and photon respectively (generated in the process).

2.2 Quark Parton Model (QPM)

Figure 2.1 shows the Feynman diagram of an electron-proton collision; with a proton p with momentum P colliding with an electron e with momentum k. On collision, the electron loses some of its energy with the emission of virtual photon γ that has a momentum q. The virtual photon then interacts with a quark in the proton resulting in a formation of a new quark, which may decay shortly after, depending on its mean life. The kinematic variables of the collision were measured using ZEUS detector at HERA.

In the quark parton model, the constituents of the proton i.e. two up quarks and one down quarks are assumed to be free and point like, called partons. Thus the electron-proton collision could be viewed as an incoherent sum of a two body that consist of elastic electron - parton, with the scattering cross section weighted by a parton density distribution function $f_i(x)$, given by Callan-Gross relations as [27],

$$F_2(x) = x\sum_i e_i^2 f_i(x) \tag{2.1}$$

and,

$$F_1(x) = \frac{1}{2x} F_2(x) \tag{2.2}$$

with x as the Bjorken scaling variable, F_1 and F_2 as the structure functions e_i as the charge of the parton, and $f_i(x)dx$ is the probability of finding a parton-i in the momentum interval of x and $x+dx$.

In the deep inelastic scattering, partons in the proton structure, the electrons and the emission of virtual photon during the interaction of the electron with the proton, could be viewed point like scattering. During the hadronisation process, the partons were ejected from the electron-proton system to form quarks after interaction with carrier(s) such as bosons, photon or gluons.

2.3 Quantum Chromodynamics (QCD)

In contrast to quark parton model (QPM), the Quantum Chromodynamic (QCD) uses non-abelian gauge theory based on the SU(3) color symmetry group field theory to explain the existence of strong interaction between the quarks. In the SU(3) color symmetry matrices, the process may undergo linear transformation of hadron on 3-dimensional complex linear space C^3. The gluons transform in the adjoint representation of SU(3), which is 8-dimensional, where the quarks are not free but interact through mediating gauge bosons called gluons , which also carry color charge themselves i.e. up (*u*), down (*d*), top (*t*), bottom (*b*), strange (*s*),charm (*c*). Here, a quark may change its flavor (*u,d,t,b,s,c*) and may split into quark and antiquark ($q\overline{q}$) through emission and absorption of gluons [7].

2.3.1 Perturbative Quantum Chromodynamics

In QCD confinement, quarks and gluons do not move freely but are bounded by strong interactions. Partons that are close together behave as free particles have a property known as Asymptotic Freedom. At small separation between the partons, where high energy probe is probable, the Perturbative Quantum Chromodynamics (pQCD) allows the observable associated with a given scattering process to be calculated, in terms of finite expansion series in a coupling constant α_s as [5],

$$f(\alpha_s) = f_1 + f_2\ \alpha_s + f_3\alpha^2 + ... \qquad (2.3)$$

The system is perturbed by the above higher order corrections, the summations run over all possible quark-gluon or gluon-gluon interactions in Feymann diagram of the system. For a Leading Order (LO), the summation runs over a single gluon emission, while a Next-to-Leading order (NLO) includes the second gluon emission or virtual gluon loop from the first gluon emission.

2.4 String Fragmentation And The Lund string Model

Due to color confinement, free quarks and antiquarks created during the electron-proton collision could not exist individually. In the Standard Model, the hadronisation process occurs when these free quarks and antiquarks combine together to form hadrons.

In Lund String Model, the hadronisation of quarks and gluons to form hadrons during the high energy electron-proton collision where free quarks were created, involves the fragmentation of color flux sring-like gluons that are binding the quarks and antiquarks ($q\bar{q}$) into hadrons. The

string of strong color field that binds the quark and antiquark may be stretched in the final state radiation, just before hadronisation took place during the electron-proton collision [39].

In the string-fragmentation scheme, the color field between the partons (i.e. quarks and gluons) may be fragmenting itself with the emission of energetic gluon carry "kinks" on the string. If the energy stored in the string is sufficient enough as when two color partons move apart, a $q\bar{q}$ pair may be created from the vacuum. The string may then break repeatedly into color singlet system for as long as the invariant mass of the string pieces exceed on-mass-shell hadrons.

The $q\bar{q}$ was created using the probability the quantum mechanical tunneling process $\exp(-\pi\, m_{q,\perp}^2 / \kappa)$, with transverse mass squared $m_{q,\perp}^2 \equiv m_q^2 + p_{q,\perp}^2$ and string tension $\kappa \approx 1\, GeV/fm$. The transverse momentum $p_{q,\perp}^2$ is locally compensated between the quark and antiquark pair. During the fragmentation, the strange and heavy-quarks production may be suppressed due to the dependence on the parton mass m_q and/or hadron mass m_h. The string-fragmentation function $f(z)$, is given by [40]:

$$f(z) \sim \frac{1}{z}(1-z)^a \exp\left(-\frac{b m_{h,\perp}^2}{z}\right) \qquad (2.4)$$

with $z = \dfrac{(E+p_{\parallel})_h}{(E+p)_q}$ as the light-cone momentum fraction

$p_{\parallel}$ as the momentum of formed hadron *h* along the direction of quark *q*

$a = 0.11$, $b = 0.54\, GeV^{-2}$ are free parameters adjustable to bring the fragmentation into accordance with measured data.

2.5 Boson Gluon Fusion

In a Deep Inelastic Scattering (DIS) process between a hadron and a lepton, the fragmentation of color partons from the DIS might produce jets of hadrons collimating around the original direction of the partons. The annihilation of leptons into a photon (or a Z^0) with subsequent production of a $q\bar{q}$ pair and the fragmentation of the $q\bar{q}$ pair into jets structure in the final state may emit a gluon with large transverse momentum relative to the parent quark [21].

In Boson Gluon Fusion (BGF), the splitting of gluon into a pair of quarks ($q\bar{q}$) with one of the quarks absorbing a virtual boson (γ^*) might result in the two jets being observed in the final states. **Figure 2.2** illustrates the BGF process of DIS of a hadron and lepton.

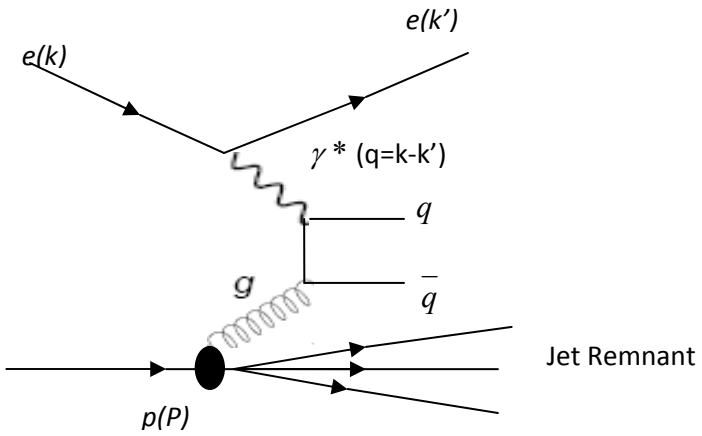

Figure 2.2 Boson Gluon Fusion (BGF) diagram from a Deep Inelastic Scattering (DIS) of a lepton and hadron

2.6 Vector Meson $\phi(1020) \rightarrow K_0^L K_0^s$

In vector meson production, the reaction $ep \rightarrow epV$, the vector meson V represented by (ρ, ω, ϕ) is often referred to as elastic scattering. The Vector meson Dominance Model (VDM) involves the scattering of photon with small virtuality $(Q^2 \approx 0)$ from the irradiation of incoming electron, with the photon acquiring a hadronic structure that allows it to fluctuate into the hadron target during *ep* interaction. At small Q^2, an ep scattering would involve two processes, namely the radiation of a virtual photon γ^* from the electron, and secondly the scattering of γ^* off the proton with an emission a struck quark from the proton (see **Figure 2.3)** [21].

The electromagnetic coupling of a photon to charge particles allows it to fluctuate into a quark and anti-quark ($q\bar{q}$) pair to interact with a parton inside the photon, when the interaction time was comparable to the lifetime of $q\bar{q}$ fluctuation of the photon [30]. The electromagnetic coupling of the photon to a bound $q\bar{q}$ state that have the same quantum number as the photon could cause the vector meson (ρ, ω, ϕ) fluctuations and scattering elastically off the incoming proton via a pomeron exchange [21] is modeled by the Vector Dominance Model (VDM). The fluctuation of photon into light vector meson production through Vector Dominance Model (VDM) is shown in **Figure 2.4**, with the elastic photon scattering off the proton via an exchange of a pomeron [21].

The coupling of a photon to a bound $q\bar{q}$ pair would add an extra component to the partonic structure of the photon. In the perturbative QCD (pQCD) model, the scattering $(\gamma * p \rightarrow Vp)$, the sequence of events were well separated in time, from the proton rest mass frame. In this model,

the photon fluctuates into a $q\bar{q}$ state that scatters on the proton target. The $q\bar{q}$ pair would later turn into a vector meson.

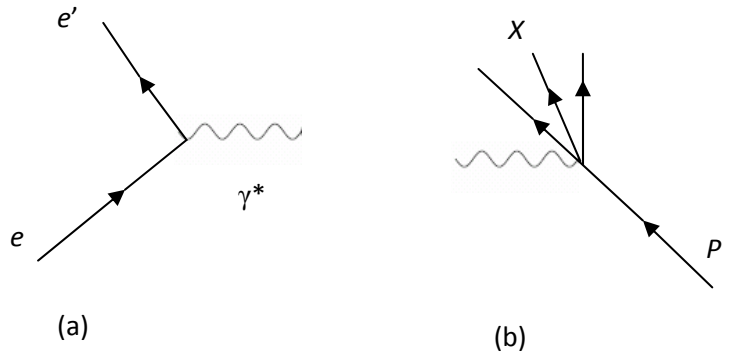

Figure 2.3 Electron-proton scattering at small Q^2, with the electron as a source of virtual photon γ* flux interacting with incoming proton resulting in hadronisation of particle X in $\gamma^* p$ interaction

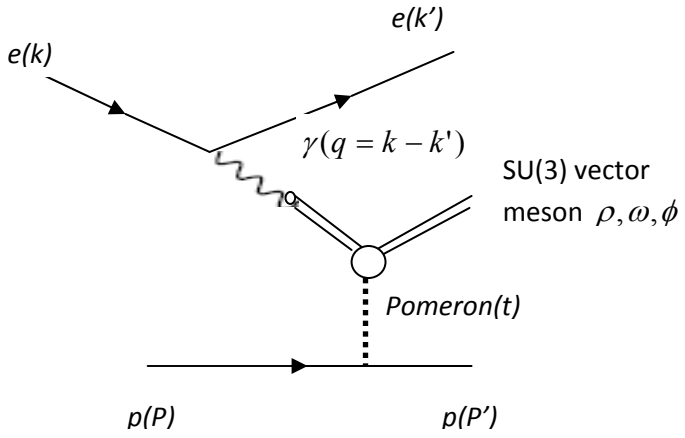

Figure 2.4 Elastic vector meson production through Vector Dominance Model (VDM), with the photon fluctuating into a vector meson, which then scatters elastically from proton via the exchange of a pomeron [21]

In **Figure 2.5**, the exclusive vector meson production through pertubative QCD model is shown, with the proton fluctuating into a $q\bar{q}$ pair with the formation of vector meson via an exchange of two gluons [21]. In the pQCD model, the production of vector meson in the presence of hard scale μ was used to probe the gluonic content of the proton.

The mixture of $u\bar{u}, d\bar{d}, s\bar{s}$ mass-eigenstates with ϕ having the most pure $s\bar{s}$ state with only a very small admixture of $u\bar{u}, d\bar{d}$ states [31].

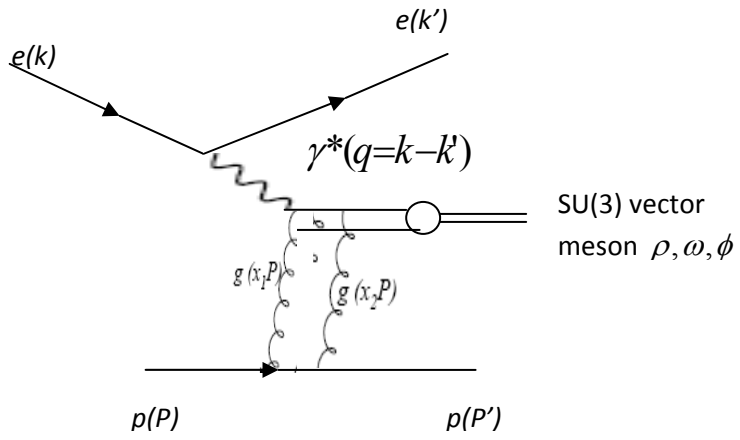

Figure 2.5 In the exclusive vector meson production based on the perturbative QCD model, the photon fluctuates into a $q\bar{q}$ pair, which then scatters off the proton to produce vector meson, via the exchange of two gluons (with momentum fraction x_1, x_2) [21]

In VDM model, when photon fluctuates into a $q\bar{q}$ pair during its interaction with a proton, the gluons transform in the adjoint representation of SU(3) during linear transformation of hadron. In case of ϕ production, the hadronisation of strange quarks could occur through the QPM model of the hard scattering of a virtual photon on the proton strange sea ($\gamma^* s \to s$), versus the first order QCD Compton (QCDC) reaction ($\gamma^* s \to sg$) or the Boson Gluon Fusion (BGF) process ($\gamma^* g \to s\bar{s}$) that depends on the gluon density in the proton [32].

For light vector mesons $q\bar{q}$ pair combinations, there are nine possible combinations of the light *u*, *d* and *s* quarks that group themselves into a nonette, as given in **Figure 2.6** The multiplets of the vector meson are classified by their strangeness *S* and isospin *I*. In the centre of nonette,

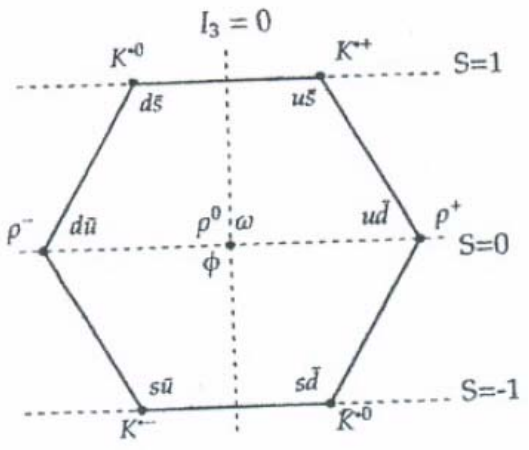

Figure 2.6 $SU(3)_{flavor}$ multiplets of light vector mesons, with various states classified by their strangeness content S and the third component I_s of their isospin [31]

2.7 Color Dipole Moment (CDM)

In QCD cascade model, the partons were treated as independent emitters of gluon. But in Color Dipole Moment (CDM) model, the gluon *g* emitted from a $q\bar{q}$ pair in an e^+e^- collision was treated as radiation of color dipole between the quark q and antiquark $\bar{q}$, with consecutive gluon emission from q and $\bar{q}$ treated as two independent qg and $\bar{q}g$ dipoles (see **Figure 2.7)** [49].

The emission phase space in color dipole model was usually plotted as in a $(\ln p_\perp, y)$ plane, with $p_\perp$ as the transverse momentum and y as the rapidity of the emitted gluon, given by[49],

$$y = \frac{1}{2}\ln\frac{1-x_1}{1-x_3} \qquad (2.5)$$

with $x_i = 2E_i / \sqrt{s_{dip}}$ as the final state energy fraction of the emitting partons in the dipole center-of-mass system s_{dip} and α_s as the effective strong coupling constant between in the incoming and outgoing struck quark.

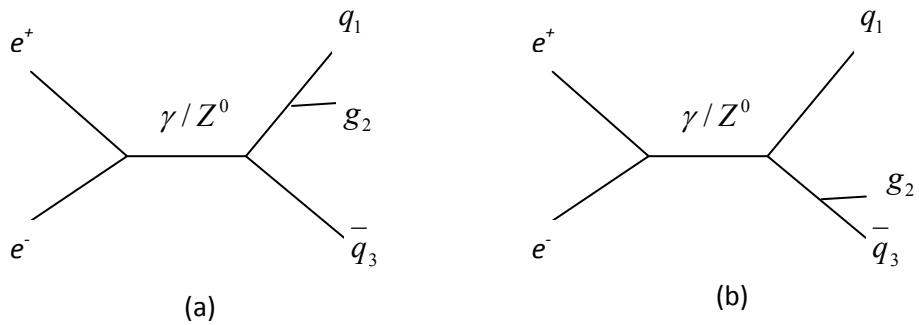

Figure 2.7 Gluon emission g_2 from a $q\bar{q}$ pair in Color Dipole Moment (CDM) model, (a) gluon emission from quark (b) gluon emission from anti-quark [49]

The cross sections of the $q\bar{q}$, qg (or $\bar{q}g$) or gg dipoles were approximated by,

$$d\sigma \propto \alpha_S \frac{dp_\perp^2}{p_\perp^2} dy \qquad (2.6)$$

The above approximation as given by CDM was only good when the emissions were strongly ordered i.e. $p_{\perp 1}^2 >> p_{\perp 2}^2 >> p_{\perp 3}^2 >>$ ....in the phase space as in **Figure 2.8a**

In CDM, the degree of freedom of the recoil partons during gluon emission was determined by the azimuthal angle ϕ of the emitted gluon and the polar angle θ of the incoming parton..

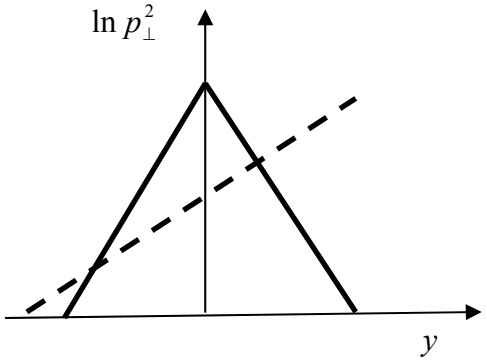

Figure 2.8a Phase space limits for emission of the first gluon (thick lines) and available space for gluon emission (dash lines) in DIS [49]

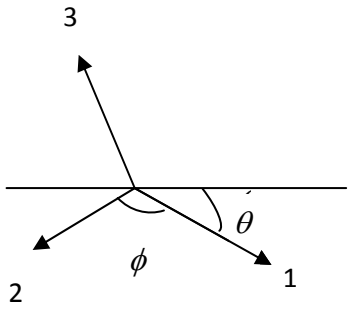

Figure 2.8b Orientation of a dipole after emission**.** azimuthal angle ϕ of the emitted gluon and the polar angle θ of the incoming parton 1

The transverse of recoils should be distributed in such manner that "the disturbance of colour flow in neighboring dipoles is minimized". In event generator Ariadne, the gluon emitted from the qg dipole always retain its direction while the gg dipole recoiled according to [49],

$$\theta = \frac{x_3^2}{x_1^2 + x_3^3}(\pi - \phi) \qquad (2.7)$$

where ϕ is the angle between parton 1 and parton 3. The azimuthal angle ϕ of the emitted gluon is assumed to be evenly distributed between 0 and 2π, with the polar angle θ of the incoming parton as in **Figure 2.8a.**

In case of the Deep Inelastic Scattering (DIS) of the electron on hadrons, CDM assumed that radiation formed between the struck quark and the hadron remnant, with the struck quark treated as point-like while the hadron remnant as extended object. Consequently, only a fraction of small wavelengths $\lambda \propto \frac{1}{p_\perp}$ from extended antenna participating in the emission. The coupling of virtual photon γ^* to a valence quark might produce colour-$\bar{3}$ charge carried by the whole remnant and is treated as simple diquark. The dipole connects to the struck quark with the valence diquark leaving a colour-less meson (with the remaining valence quark and anti-sea-quark). In case of dipole connecting to the anti-sea-quark, a baryon is produced instead. The hadron carries with it a fraction of z of the original proton from the Lund symmetric function.

In the remnant treatment involving "gluonic" object pomeron (such as the production of ϕ meson in Vector Dominance Model (VDM)), the virtual photon γ^* cannot couple directly to a "gluonic" object pomeron . Here, the remnant is treated as extended gluon connecting both the quark and the corresponding antiquark with one dipole each . The "pomeron-induced" part of the total parton density function $f_q^p(x, Q^2)$ is given by a simple convolution [49],

$$f_q^{p(IP)}(x,Q^2) = \int dt \int dz \int dx_{IP}\ f_{IP}^{p}(x_{IP},t)\ f_q^{IP}(z,Q^2)\ \delta(zx_{IP} - x) \qquad (2.8)$$

with $f_{IP}^{p}(x_{IP},t)$ as the pomeron flux taking a fraction x_{IP} of the proton momentum transfer *t* with density of quarks $f_q^{IP}(z,Q^2)$ within the pomeron and, z as the fraction of the original proton momentum in the Lund symmetric fragmentation function.

In this case, the pomeron remnant is the antipartner of the struck quark. For the struck quark be part of the pomeron, the probability $f_q^{p(IP)}(x,Q^2) / f_q^{P}(X,Q^2) < 1$ will result in the dipole between the struck quark and the pomeron remnant.

2.8 Kinematic Variables of the Electron-Proton Collision

In an electron-proton collision, a proton *p* beam accelerated in the positive z-axis, at a momentum P, collided with an electron *e* beam at momentum *k* in the opposite direction of the proton beam. After the collision, the electron is scattered with momentum k' at angle θ_e from its original direction (as in **Figure 2.9**), while the proton is scattered with momentum P' from its initial direction. During a deep inelastic scattering (DIS), a fraction of electron momentum maybe lost through a photon (real γ or virtual γ*) though the exchange of a boson.

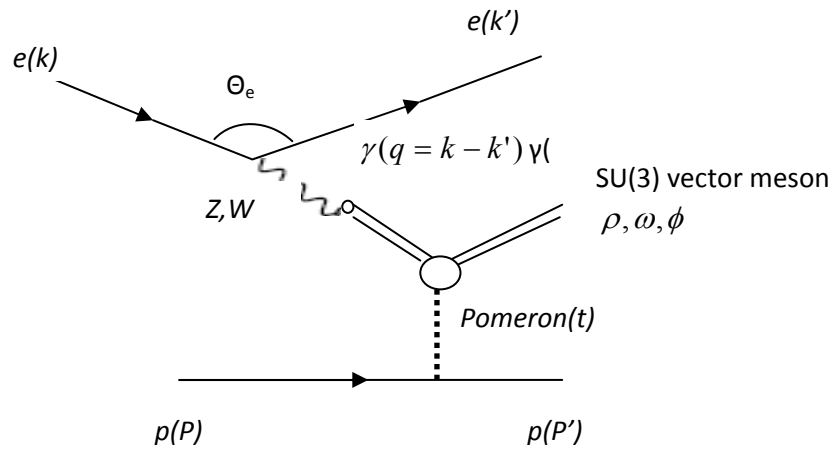

Figure 2.9 Kinematic variables in the electron-proton collision, with P, k , q as the momentum of proton *p*, electron *e*, and photon *γ* respectively (generated in the process). The production of ϕ meson via a promeron exchange an virtual photon γ in the vector meson model (VDM)

Assuming that the mass of the incoming and scattered electron were negligible, the centre-of-mass energy *s*, of the e-p system is given by,

$$s = (k + P)^2 \approx 4E_e E_p \qquad (2.9)$$

where E_e (=30GeV) and E_p (=920GeV) are energies of incoming electron and proton respectively. The centre-of-mass W^2, for the intermediate boson-proton is given by,

$$W^2 = (q + P)^2 \qquad (2.10)$$

During the interaction, the photon, whether real γ or virtual γ*, gains momentum from the incoming electron through the following relation,

$$Q^2 = -q^2 = -(k - k')^2 \qquad (2.11)$$

with *k* as the four-momentum of initial electron and *k'* as the four-momentum of electron emerges from the scattering.

In deep inelastic scattering (DIS) where the struck quark from the proton carries with it a fraction x of the incoming proton's momentum as given by the Bjorken scaling x,

$$x = \frac{Q^2}{2p.q} \tag{2.12}$$

In the rest frame of the proton, the inelasticity y (i.e. fraction of the electron's energy transferred to the proton) reduces to:

$$y = \frac{E_e - E_{e'}}{E_e} = 1 - \frac{E_{e'}}{E_e} \tag{2.13}$$

with E_e as energy of the incoming electron and $E_{e'}$ as energy of the outgoing leptons

2.9 Kinematic Variables of Hadrons in the Final States

During the electron-proton collision in the ZEUS detector at HERA, some particles that emerged from the interaction might travel the whole length of ZEUS detector to deposit their island of energies as in the electromagnetic calorimeter (EMC) and hadronic calorimeters (HAC) of the ZEUS detector. Such particles were identified as either charged through their association with tracks that were formed in their trajectories in the ZEUS detector, or as neutrals if there was no track associated with the energy islands.

Assuming that an object-i in the final state states that travels to the calorimeter of the ZEUS detector has a four-momentum $p_i = (p_{xi}, p_{yi}, p_{xi}, E_i)$, that makes a polar angle θ_i with the z-axis and azimuthal angle ϕ_i in the x-y plane is shown in **Figure 2.10**.

Using the momentum in the x-y-z direction, the polar angle θ_i of particle-i is given by,

$$\cos\theta_i = p_{xi}^2 / (p_{xi}^2 + p_{yi}^2 + p_{zi}^2) \qquad (2.14)$$

with its azimuthal angle $\cos\phi_i$ of object-i, as

$$\cos\phi_i = p_{xi}^2 / (p_{xi}^2 + p_{yi}^2) \qquad (2.15)$$

In the ZEUS detector, the momentum of uncharged tracks of object-i was calculated by assuming object-i as pions. Thus, we could use the equation (2.6) above to calculate the direction of uncharged object-i without from the ZUFOS entry data in the Orange ntuple blocks of the ZEUS analysis code.

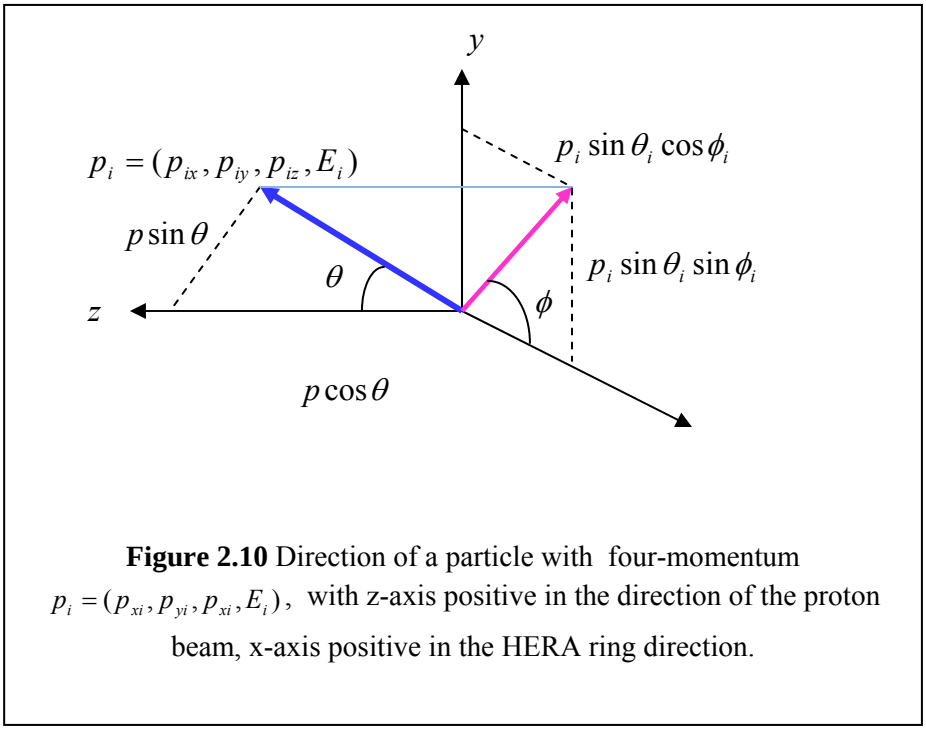

Figure 2.10 Direction of a particle with four-momentum $p_i = (p_{xi}, p_{yi}, p_{xi}, E_i)$, with z-axis positive in the direction of the proton beam, x-axis positive in the HERA ring direction.

In the calorimeter of the ZEUS detector, the energy clusters of cells in the calorimeter that was not associated with any track and not part of the calorimeter objects considered as neutral energy, with the neutral object energy E related to its momentum by $E^2 = p^2$ [27].

In this case, virtual photon produced by the incoming electron in electron-proton collision contributed totally to the formation of neutral particle when the virtual photon, as given in **Equation (2.11)**, strike a quark from a proton through a pomeron as given in Vector Dominance Model (VDM) model. In this limit, the particle is travelling close to the speed of light, the approximation of the mass of the particle is nearly zero or $m \to 0$.

Assuming that the particle-i with energy E_i travel towards the calorimeter of the ZEUS detector and deposits its energy along the trajectory. As the momentum p_i of object-i is proportional to its E_i, therefore the components of p_i in x, y and z-axis would also be proportional to its energy E_i, the transverse momentum is reduced to [6]:

$$p_T = \sqrt{p_x^2 + p_y^2} = \sqrt{(E_T \cos\phi)^2 + (E_T \sin\phi)^2} \approx E_T = E \sin\theta \qquad (2.16)$$

Thus the kinematic variables of the object-i traveling close to the speed of light and exist in the final states, in terms of the momentum components (p_{xi}, p_{yi}, p_{zi}) and energy E_i, could be written as the following [15],

(i) The momentum p_i of object-i, in terms of energy deposit E_i, polar angle θ_i and azimuthal angle $\cos\phi_i$ of object-i [15] ,

$$p_{xi} = E_i \sin\theta_i \cos\phi_i \qquad (2.17)$$

$$p_{yi} = E_i \sin\theta_i \sin\phi_i \qquad (2.18)$$

$$p_{zi} = E_i \cos\theta_i \tag{2.19}$$

$$p_i = \sqrt{(E_i \sin\theta_i \cos\phi_i)^2 + (E_i \cos\theta_i \sin\phi_i)^2 + (E_i \cos\theta_i)^2} \tag{2.20}$$

(ii) Transverse momentum of object-i;

$$p_{Ti}^2 = p_{xi}^2 + p_{yi}^2 = E_i(\sin\theta_i \cos\phi_i)^2 + (E_i \sin\theta_i \sin\phi_i)^2 \tag{2.21}$$

(iii) Invariant mass of object-i,

The invariant mass of the hadronic in the final state, from its measured four-momenta, is given by $mass_i = \sqrt{E_i^2 - p_{xi}^2 - p_{yi}^2 - p_{zi}^2}$ [13], Substituting **Equations (2.17), (2.18)** and **(2.19)** into this equation would give the invariant mass of object-i, in terms of is energy, azimutal and polar angles as:

$$mass_i = \sqrt{E_i^2 - (E_i \sin\theta_i \cos\phi_i)^2 - (E_i \sin\theta_i \sin\phi_i)^2 - (E_i \cos\theta_i)^2} \tag{2.22}$$

(iv) $$\delta_i = E_i - p_{zi} = E_i(1 - \cos\theta_i) \tag{2.23}$$

(v) Rapidity: $$y_i = \frac{1}{2}\ln\left(\frac{E_i + p_{zi}}{E_i - p_{zi}}\right) = \frac{1}{2}\ln\left(\frac{E_i + E_i\cos\theta_i}{E_i - E_i\cos\theta_i}\right) \tag{2.27}$$

(vi) Pseudorapidity: $$\eta_i = -\ln\left(\tan\frac{\theta_i}{2}\right) \tag{2.28}$$

(vii) Ratio p_{Ti} / p_i from energy

$$\frac{p_{Ti}}{p_i} = \sqrt{\frac{(E_i \sin\theta_i \cos\phi_i)^2 + (E_i \sin\theta_i \sin\phi_i)^2}{(E_i \sin\theta_i \cos\phi_i)^2 + (E_i \sin\theta_i \sin\phi_i)^2 + (E_i \cos\theta_i)^2}} \tag{2.29}$$

In the study on neutral and charge current (NCC) cross section at high Q^2 at HERA, the summed the momentum as given in **Equations (2.17), (2.18)** and **(2.19)** was used for all cells in

the calorimeter of the ZEUS detector [17]. The **Equations (2.17), (2.18) and (2.19)** was also used to calculate the momentum of the scattered positron in the measurement of dijet cross sections with a leading neutron in photoproduction [9] and the four momentum of scattered electron in the measurement of hadron in final state in diffractive DIS tagged with leading proton spectrometer [13].

From the invariant mass equation of object-i, i.e. $m_i^2 = E_i^2 - p_i^2$, the ratio of the four-momenta p_i of object-i to its energy E_i is given by

$$\frac{p_i}{E_i} = \sqrt{1 - \frac{m_i^2}{E_i^2}} \qquad (2:30)$$

2.9.1 Deep Inelastic Scattering (DIS)

In the deep inelastic scattering (DIS) of the electron-proton collision, the kinematics of DIS for particles is as the follows:

The electron method:

$$Q_i^2 = 2E_{ei}E_{ei}^{'}(1+\cos\theta_{ei}) \qquad (2.31)$$

$$y = 1 - \frac{E_e^{'}}{2E_e}(1-\cos\theta_i) \qquad (2.32)$$

$$x = \frac{Q^2}{sy} \qquad (2.33)$$

At relatively low Q^2 ($Q^2 < 100\ GeV^2$), the reconstruction variables using electron methods is recommended as it has better resolution [28].

At relatively low Q^2 ($Q^2 < 100\ GeV^2$), the reconstruction variables using electron methods is recommended as it has better the best resolution [28].

The hadron method/Jacquet-Blondel method:

$$\delta = \sum_{i=1}^{\#hadronss} E_i(1-\cos\theta_i) = E_{had} - p_{z,had} \tag{2.34}$$

$$y_{JB} = \frac{\delta_{had}}{2E_e} \tag{2.35}$$

$$x_{JB} = \frac{Q^2}{sy_{JB}} \tag{2.36}$$

$$W_{JB} = \sqrt{y_{JB}\ s} \tag{2.37}$$

The Jacquet-Blondel method relies entirely on measurements of the hadronic system under study.

The Double Angle Method:

$$\cos\gamma = \frac{p_{T,had}^2 - \delta_{had}^2}{p_{T,had}^2 + \delta_{had}^2} \tag{2.38}$$

$$Q^2 = 4E\frac{\sin\gamma(1+\cos\theta_e)}{\sin\gamma + \sin\theta_e - \sin(\theta_e+\gamma)} \tag{2.39}$$

$$x = \frac{E_e}{E_p}\frac{\sin\gamma + \sin(\theta_e+\gamma)}{\sin\gamma - \sin(\theta_e+\gamma)} \tag{2.40}$$

In Double Angle Method, the angles of scattered positron and hadronic energy flow are used.

2.10 Long Live Neutral Hadrons in Final States

2.10.1 K_L^0 Production

In the deep inelastic scattering of the electron-proton collision, the sea of strange (s) quarks in the proton may result in the production of ϕ meson. In terms of Quark Parton Model (QPM), a hard scattering of virtual photon on a proton consisting of strange sea of quarks through reaction $\gamma * s \to s$ could result in the hadronisation of the strange quarks to produce ϕ meson. Other source of the strange quarks is the QCD Compton (QCDC) through $\gamma * s \to s\, g$ in the first order of QCD process, and the Boson Gluon Fusion (BGF) through $\gamma * s \to s\bar{s}$ reaction [28] in the first order of QCD process. In contrast to the QPM and QCDC process, the BGF events are determined by the gluon density in the proton [28].

Thus, the production of ϕ meson (as the source of K_L^0 and K_S^0 through $\phi \to K_L^0 K_S^0$ decay channel) could provide information on the strange quark production through the hard photon scattering on a sea of strange quarks in the proton. The study of $K_L^0 K_S^0$ production has been carried out using e^+e^- annihilation process and the Vector Dominance Model (VDM) to search for excitations of the $\rho(770),\ \omega(780),\ \phi(1020)$, where the vector mesons with isospin $I = 0, I = 1$ decayed into a kaon pair [34].

In the DIS of the e-p system, the hadronisation of the strange quarks during hard interaction could produce ϕ-meson. The study on the ϕ-meson production in DIS and its sensitivity to strange sea quarks in the proton has been carried out by [28] in Breit frame where the exchanged

virtual boson is virtuality Q was completely space-like, with radiation of the outgoing struck quark and the proton remnant clearly separated.

With the ϕ-meson in nearly a pure $s\bar{s}$ state due to ideal mixing with the ω and the contribution from resonance decay was small, the sensitivity of ϕ-meson cross sections to strange sea of quarks in the proton was expected to be higher than the K^0 $(d\bar{s})$ mesons and Λ (uds) baryons . Thus, the measurements of ϕ-meson with high transverse momentum p_T that minimize contribution from fragmentation, could provide information on strange quark production by hard interaction with strange sea of quarks in the proton [28].

Figure 2.11 shows the $\phi \to K_L^0 K_S^0$ decay channel, with K_L^0 and K_S^0 in the opposite direction to preserve the ϕ momentum. In this decay K_L^0 with decay length of 15.33m and mean life of $(5.114 \pm 0.021) \times 10^{-8} s$ [35], any K_L^0 produced would proceed to the hadronic calorimeter of the ZEUS detector, while K_S^0 would decay in the immediately after being produced (with mean life of $(0.8958 \pm 0.0006) \times 10^{-10} s$ and decay length 206842cm) detectable by the central tracking detector (CTD) of the ZEUS detector.

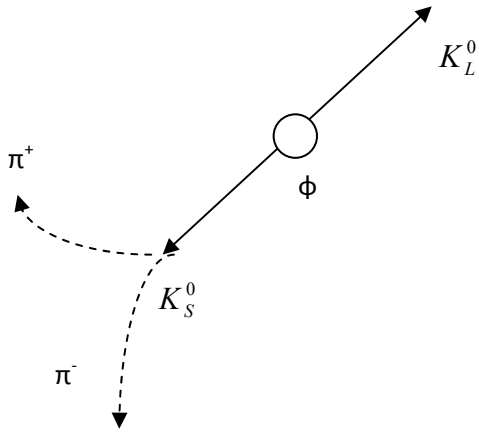

Figure 2.11. An exclusive ϕ decay through $\phi \to K_L^0 K_S^0$. $\phi \to K_L^0 K_S^0$ channel has 34.0% yield, with $K_S^0 \to \pi^+ \pi^-$ yield 69.2%

2.10.2 Leading Neutron production at HERA

Neutron and proton are the most common baryon members naturally found in the universe, with proton and neutron as the most common hadrons and are stable with mean life of $> 1.9 \times 10^{29}$ years and 885.7 seconds, respectively.

Neutrons and proton has three quarks each, with proton having two up (u) quarks and one down (d) quark and, neutrons with one up (u) and two down (d) quarks. These quarks are held together in proton and neutron by strong force mediated by gluons. As fermions, the quarks and leptons have (intrinsic angular momentum) spin ½. In the composite particles the quarks combine together to from hadrons with one spin as a whole.

Neutrons and proton as members in baryon family with baryon number B, define as:

$$B = \frac{n_q - n_{\bar{q}}}{3} \tag{2.41}$$

with n_q as the number of constituent quark and $n_{\bar{q}}$ as the number of constituent antiquarks

The production of leading neutron *n* during the dijet photoproduction events at HERA has been associated to the virtual photon produced during the interaction of proton-electron collision in the following process [37]:

$$e^+ + p \rightarrow e^+ + jet + jet + X + n \tag{2.42}$$

Leading neutron production has been studied using the Forward Neutron Calorimeter (FNC), located 105.6m downstream the HERA tunnel in the proton direction [38], where the leading neutrons, which carried majority of the energy from the electron-proton collision, moved in straight trajectory as the incoming protons, and was detected at the FNC (Forward Neutron Calorimeter) [38].

Figure 2.12 gives the schematic diagram of resolved photoproduction of dijets in leading neutron mediated by meson exchange, with x_π (x_γ) denotes the fraction of energy exchanged meson (photon) participating the partonic hard scattering, with σ as the hard cross section involved. In case of direct photoproduction and no photon remnant, $x_\gamma = 1$ with the photon behave in point like manner [37].

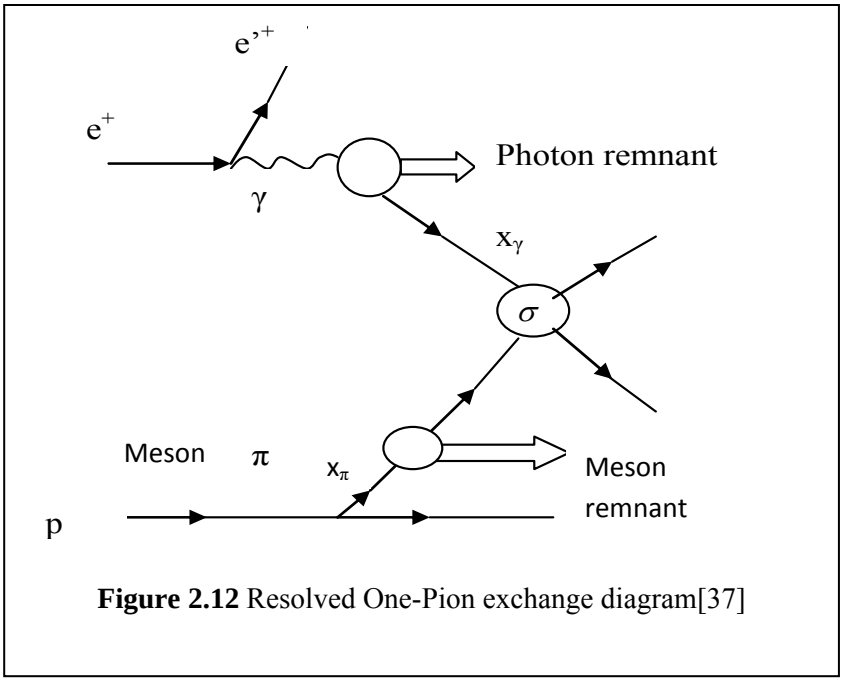

Figure 2.12 Resolved One-Pion exchange diagram[37]

2.10.3 Neutron production through $\Lambda \to n\pi^o$ channel

The neutral strangeness production study at the ZEUS detector has been carried out using the inclusive production of neutral strange particle to provide insights to the fragmentation process of $\Lambda, \overline{\Lambda}, K_S^0$ in the *ep* collision [7].

While the previous study of $\Lambda \to p^+\pi^-$ fragmentation (**Figure 2.13a**) was used with ZEUS central tracking detector (CTD), in this thesis, the fragmentation of Λ through the $\Lambda \to n\pi^0$ channel was used. **Figure 2.13b** gives the schematic diagram of fragmentation of $\Lambda \to n\pi^0$, where the neutron being produced moves in straight direction through EMC (electromagnetic calorimeter) to HACs (hadronic calorimeter) of the ZEUS detector, and the undetected (i.e.

uncharged tracks) by the CTD. As π^0 is unstable, it decays into two photons moving in the same direction of π^0 and depositing 95% of its energy in the EMC of the ZEUS detector.

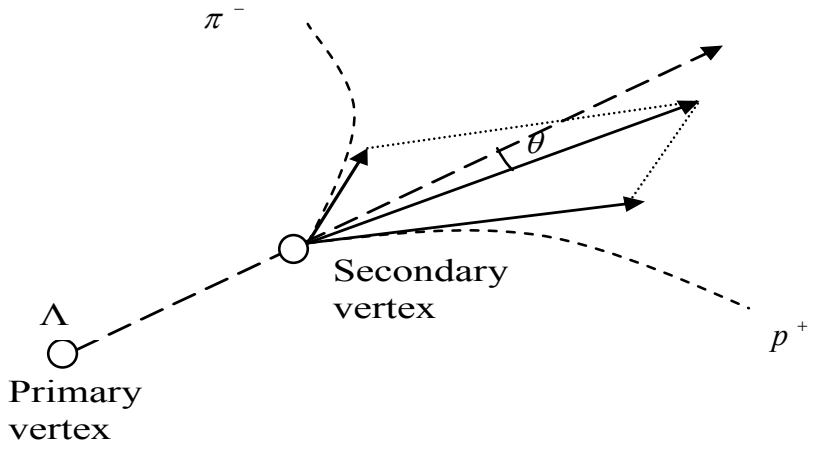

Figure 2.13a An Example of Λ^0 decay through $\Lambda^0 \to \pi^- p^+$ channel, where the two decay products moved apart in electromagnetic field in CTD., leaving two detectable tracks[7]. The yield is 63.9%.

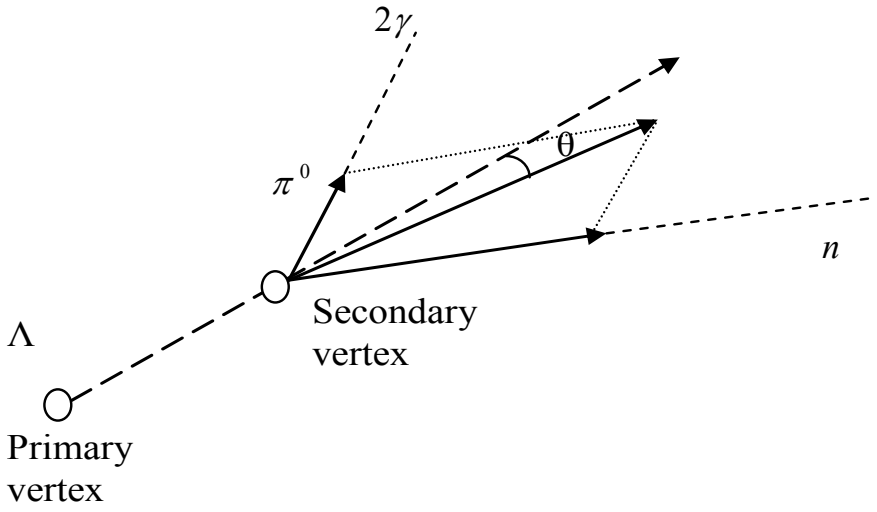

Figure 2.13b An Example of Λ^0 decay through $\Lambda \to n\pi^0$ channel (35.8% yield) where the two decay products moved along its original trajectories in two undetectable tracks, with $\pi^0 \to 2\gamma$ (98.8%).

The advantage of using $\Lambda \to n\pi^0$ channel is that the study of CP (Conjugate and Parity) could be carried out using the radial distribution of neutral particles where charges of both mother and decay products were conserved – only the states changes involve i.e. (uds) in Λ to (udd) in n and $(u\bar{d})$ in π^0 .

In this thesis, we attempt to find neutrons in mode $\Lambda \to n\pi^0$ above, using data with uncharged track that form islands in the HAC (hadronic calorimeter) cells of the ZEUS detector, using ZUFOs (Zeus Unidentified Flow Objects) blocks in the ntuples.

2.11 Conservation of Strangeness Number

In 1947, when the process of $\Lambda \to n\pi^0$ was first observed, the fact that Λ has much longer life time (i.e. $10^{-10} s$) than expected ($10^{-23} s$) due large mass and large production cross section.

This observation lead to the term "strangeness conservation" where the baryon Λ preserve the strangeness number S = -1, in such a way that strange quark s must be transformed in a process that can only occur through weak interaction that leads to longer life time.

In case of the ϕ (1020) meson, its nearly pure state of $s\bar{s}$ due to ideal mixing with ω and the contribution of resonance decay to the ϕ meson production is small makes it a good choice for studying the strange sea in the proton. Previous works of on inclusive ϕ (1020) meson production at HERA has been carried out in the virtuality of exchange photon range $10 < Q^2 < 100\, GeV$ using the decay $\phi \to K^+K^-$ channel to study the hard scatterings on an $s\bar{s}$ pair leading to the production of a ϕ meson in the Breit frame to separate the radiation of the outgoing struck quark and the proton remnant [28].

The inclusive production of strange particle $\Lambda, \overline{\Lambda}$ using the $\Lambda \to p\pi^-$ at high Q^2 in DIS has been carried out at HERA to study the fragmentation in ep collision [7].

In this thesis, the decay of $\Lambda \to n\pi^0$ involving the strange quark s component in baryon $\Lambda\,(uds)$ and the decay of light unflavored meson ϕ into strange mesons K_S^0 and K_S^0 through decay channel $\phi \to K_L^0 K_S^0$ will be used to provide additional information on the initial state of state Λ and ϕ during the electron-proton collision in the ZEUS detector by tracking the dynamics of their respective decay products, namely n, π^0 and K_L^0, K_S^0, with n and K_L^0 in their hadronic final states. **Table 2.1** and **Table 2.2** give the properties of $\Lambda \to n\pi^0$ and $\phi \to K_L^0 K_S^0$ channel respectively.

Table 2.1 Components of $\Lambda \to n\pi^0$ channel

Decay scheme	$\Lambda \to n\pi^0$		
particle	Λ	n	π^0
Quark components	uds	udd	$\frac{\bar{u}u + \bar{d}d}{\sqrt{2}} \approx u\bar{d}$
Strangeness	-1	0	0
$I(J^P)$	$0\left(\frac{1^+}{2}\right)$	$\frac{1}{2}\left(\frac{1^+}{2}\right)$	
$I^G(J^{PC})$			$1^-(0^{-+})$

C : charge conjugation, P: Parity, G: parity on whole multiplet

Table 2.2. Components of $\phi \to K_L^0 K_S^0$ channel

Decay scheme	$\phi \to K_L^0 K_S^0$		
particle	ϕ	K_L^0	K_S^0
Quark components	$c_1(u\bar{u} + d\bar{d}) + c_2(s\bar{s}) \approx s\bar{s}$	$d\bar{s}$	$d\bar{s}$
Strangeness	-1		
$I^G(J^{PC})$	$1^-(0^{++})$		
$I(J^P)$		$\frac{1}{2}(0^-)$	$\frac{1}{2}(0^-)$

C : charge conjugation, *P*: Parity, *G*: parity on whole multiplet